Modelling Heat and Mass Transfer in Wood-frame Floor Assemblies Exposed to Fire

STEVEN T. CRAFT[1,2], BURKAN ISGOR[2], JAMES R. MEHAFFEY[1], and GEORGE HADJISOPHOCLEOUS[2]
[1]Building Systems – Fire Program
FPInnovations – Forintek Division
Suite 4100 – CTTC, 1125 Colonel By Drive, Ottawa, ON, CANADA, K1S 5R1
[2]Civil and Environmental Engineering
Carleton University
1125 Colonel By Drive, Ottawa, ON, CANADA, K1S 5B6

ABSTRACT

A two-dimensional finite-element model has been developed to simulate the heat and mass transfer in both gypsum board and wood in order to predict the thermal response of a wood-frame floor assembly exposed to fire. Both volatile pyrolysis products in wood and water vapour in wood and gypsum board are considered in the mass transfer analysis. Calcination of gypsum board and pyrolysis of wood are modelled using Arrhenius expressions. The evaporation of water is modelled assuming the partial pressure of water is equal to the equilibrium vapour pressure. The gas in the cavity is assumed to be fully transparent, allowing radiant heat transfer between all surfaces in the cavity, thus leaving convective heat transfer to heat the gas inside the cavity.

Comparisons are made to two full-scale fire resistance tests. One test was carried out using the standard temperature exposure while the second test used a non-standard exposure that was based on measurements taken in experimental fires in wood frame houses. Comparisons between experiment and model predictions show good agreement on the unexposed side of each of the two layers of gypsum board protecting the assembly. The cavity temperature is under-predicted resulting in an under-prediction of the temperatures in the floor joist and sub-floor. The model currently does not account for the fall-off of gypsum board which limits the models ability to predict the results for the non-standard exposure since the gypsum board failed very early in the test.

KEYWORDS: modelling, heat transfer, mass transfer, protection of wood, gypsum board

NOMENCLATURE LISTING

A	surface area, m^2
c	specific heat, J kg^{-1} K^{-1}
c_v	specific heat at constant volume, J kg^{-1} K^{-1}
D	permeability, m^2
$F_{S\text{-}S2}$	configuration factor between surface and opposing surface
h	convective heat transfer coefficient, W m^{-2} K^{-1}
k	thermal conductivity, W m^{-1} K^{-1}
$\dot{m}''$	mass flux, kg m^{-2} s^{-1}
$\dot{m}'''_{GEN}$	rate of generation of vapour per unit volume, kg m^{-3} s^{-1}
M_w	molecular weight, kg mol^{-1}
P	pressure, Pa
$\dot{q}''_{cavity}$	net heat flux on surface inside cavity, W m^{-2}
$\dot{Q}'''_{EVAP}$	rate of absorption of heat per unit volume due to evaporation of water, W m^{-3}
$\dot{Q}'''_{HR}$	rate of absorption of heat per unit volume due to chemical reactions, W m^{-3}
R	gas constant, J K^{-1} mol^{-1}
T	temperature, K
t	time, s

FIRE SAFETY SCIENCE–PROCEEDINGS OF THE NINTH INTERNATIONAL SYMPOSIUM, pp. 1303-1314
 / DOI:10.3801/IAFSS.FSS.9-1303

Greek

ε	emissivity
ρ	unit mass, kg m^{-3}
σ	Stefan-Boltzmann constant, W m^{-2}, K^{-4}
υ	kinematic viscosity, m^2 s^{-1}
φ	porosity, m^3 m^{-3}

subscripts

air	air inside the cavity
S	surface facing the cavity
S2	opposing surface within cavity
∞	ambient condition

INTRODUCTION

The fire safe design of buildings built in Canada has traditionally been met by following a prescriptive building code. With the introduction of an objective based code in 2005, in Canada it is now possible to construct a building that deviates from the prescriptive code but meets its objectives, provided the alternative design is as safe as the prescriptive solution. It is, therefore, necessary to be able to determine the risk to life and property of prescriptive and alternative designs in order to make the comparison. In order to compare the fire risk of alternative designs to life and property, Carleton University has developed a risk model [1] for four story, wood-frame buildings. A number of submodels are needed in order to be able to calculate the overall risk due to fire. For example, submodels are used to characterize fire growth, smoke movement, occupant response and movement. Another important submodel characterizes the response of the assembly to fire, which is the focus of this paper. This submodel provides information to the risk model that may affect fire spread between compartments as well as smoke movement and potentially occupant movement. Unfortunately, the standard fire-resistance test, CAN/ULC S101 [2] or ASTM E119 [3], used to evaluate assemblies for code compliance does not provide the necessary information to predict the response of an assembly subjected to alternative exposures resulting from different fire scenarios. While alternative testing could provide the information needed, the expense and number of tests required cause it to be uneconomical. Therefore, the best solution is computer modelling.

A number of models have been developed in the past 15 years that predict the response of a wood-frame assembly to the standard fire resistance test [4-7]. The main challenge in modelling wood assemblies protected by gypsum board is the lack of robust material property data for wood and gypsum board at elevated temperatures. As a result of this, the models previously developed made simplifications to account for phenomena not easily modelled. For instance, thermal conductivity was typically calibrated in an attempt to account for mass transfer, and the energy associated with evaporation and chemical reactions was included in the specific heat. These simplifications work well in the standard fire-resistance test where the exposure temperature increases monotonically at a specified rate. For scenarios that differ from the standard fire test, such as those with a rapid heating phase followed by a cooling phase, better representation of the thermal degradation of gypsum board and wood are required in order to accurately model the performance of these assemblies.

A two-dimensional heat and mass transfer finite-element model has been developed in order to more precisely predict the response of a wood-frame floor assembly exposed to fire. The heat and mass transfer analyses are coupled since the mass transfer contributes to heat transfer and the heat transfer is what ultimately drives the mass transfer. The mass transfer contributes to heat transfer through the movement of water vapour and pyrolysis products in the case of wood. The heat transfer causes a pressure rise due to evaporation of water and the release of pyrolysis products in wood which creates pressure gradients and subsequent mass transfer.

The objective of this paper is to present the predictions of the heat and mass transfer model for full-scale fire-resistance tests conducted on wood-frame floor assemblies.

MODEL DESCRIPTION

A two-dimensional finite-element model has been developed to model the heat and mass transfer in both gypsum board and wood as components of a wood-frame floor assembly [8]. The model methodology is based on that used by Fredlund [9]. The model allows the material properties of each material to vary as a function of temperature or as a function of another property. Chemical reactions are simulated using Arrhenius expressions and evaporation of water is determined based on temperature and pressure. A cross-section of the floor assembly is shown in Fig. 1 with the shaded portion representing the area considered in the model.

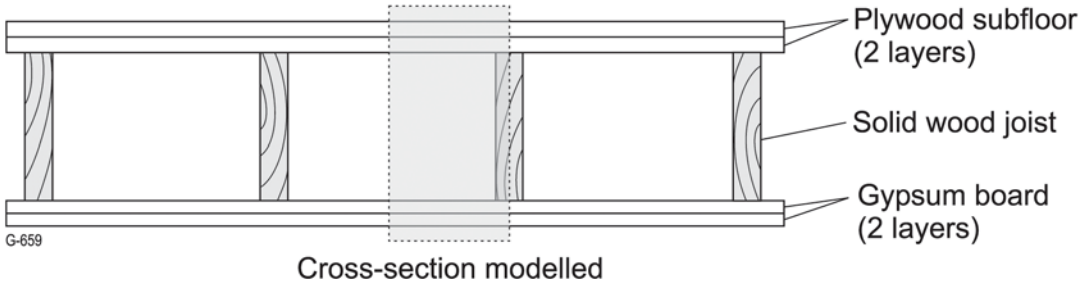

Fig. 1. Cross-section of floor assembly with shaded region indicating area considered in model.

Conservation of Energy

The heat transfer analysis includes both conductive and convective heat transfer in the solid material. The convective heat transfer is determined from the mass transfer analysis and includes the movement of water vapour and volatile pyrolysis products in wood, and water vapour in gypsum board. The following equation represents the conservation of energy used in the analysis.

$$-\nabla\cdot\left(-\,k\,\nabla T\right)-\dot{m}''\,c_v\cdot\nabla T+\dot{Q}'''_{EVAP}+\dot{Q}'''_{HR}=\rho\,c\,\frac{\partial T}{\partial t} \qquad (1)$$

The first term on the left represents conductive heat transfer (Fourier's law) where k is the thermal conductivity and T is temperature. The second term is the convective heat transfer within the material where $\dot{m}''$ is mass flux of water vapour and pyrolysis products and c_v is the specific heat of the gas at constant volume. The third term, $\dot{Q}'''_{EVAP}$, is the rate of absorption of heat per unit volume due to evaporation of water, and the fourth term, $\dot{Q}'''_{HR}$, is the rate of absorption of heat per unit volume due to pyrolysis in wood and calcination of gypsum in gypsum board. The term on the right side represents the rate of change of accumulated energy in the material where ρ is unit mass, c is specific heat and t is time.

Heat Transfer Boundary Conditions

Heat is transferred to the gypsum board ceiling of the floor assembly from the hot furnace gases and lining through convection and radiation. Similarly, heat is lost from the sub-floor on the top of the floor assembly to the surroundings through convection and radiation.

The heat transfer within the cavity in the floor assembly is calculated assuming the gas inside the cavity is fully transparent. Therefore, heating of the cavity air is through convection only. In order to calculate the change in temperature in the cavity from one time-step to the next, an iterative solution is used to solve an energy balance for the cavity. The following equation represents the energy balance solved.

$$\sum_{\text{Each Surface}}\left[h\,A\left(T_S-T_{air}\right)\right]=\rho_{air}\,c_{air}\,\frac{\partial T_{air}}{\partial t} \qquad (2)$$

Where the convective component on the left hand side is summed over all surfaces inside the cavity, h is the convective heat transfer coefficient, A is the surface area, T_S is the surface temperature, T_{air} is the cavity air temperature, ρ_{air} is the density of the air in the cavity, c_{air} is the specific heat at constant pressure of the air in the cavity and t is time.

The net radiative flux on the surface in the cavity is calculated by summing the radiation between the surface and all other surfaces that "see" each other. The following equation represents the boundary condition inside the cavity.

$$\dot{q}''_{cavity} = hA\left(T_S - T_{air}\right) + \sum_{EachSurface} F_{S-S2}\sigma\varepsilon\left(T_{S2}^4 - T_S^4\right) \quad (3)$$

Where $\dot{q}''_{cavity}$ represents the heat flux seen at the surface inside the cavity, the first term on the right hand side of the equation represents the convective heat transfer, and the second term on the right represents the radiative heat transfer. Within the radiation term, the radiation is summed between the surface and all other surfaces it "sees", F_{S-S2} is the configuration factor between the surfaces, σ is the Stefan Boltzman constant, ε is the emissivity, T_S is the surface temperature and T_{S2} is the temperature of the opposing surface.

Conservation of Mass

The mass transfer analysis models the pressure-driven flow of water vapour and volatile pyrolysis products in wood, and water vapour in gypsum board for input into the heat transfer analysis. The following equation represents the conservation of mass used in the analysis.

$$-\nabla\cdot\left(-\frac{D}{\upsilon}\nabla P\right) + \frac{\varphi M_W}{R\,T^2}\frac{\partial T}{\partial t}P + \dot{m}'''_{GEN} = \frac{\varphi M_W}{R\,T}\frac{\partial P}{\partial t} \quad (4)$$

The first term on the left represents pressure-driven flow governed by Darcy's Law where D is the permeability, υ is the kinematic viscosity and P is pressure. The second term accounts for the increase/decrease in pressure of gas due to a change in temperature where φ is the porosity, M_W is the molecular weight and R is the gas constant. The third term, $\dot{m}'''_{GEN}$, is the rate of generation/reduction of water vapour due to evaporation/condensation per unit volume and the rate of generation of volatile pyrolysis products per unit volume in the case of wood. The term on the right side represents the rate of change of mass of gas in the pores of the material.

Mass Transfer Boundary Conditions

Mass transfer at the boundaries is modelled assuming the pressure on the surface of the material is atmospheric. This includes all exposed and unexposed surfaces (i.e. between layers of gypsum board and between the gypsum board and the solid wood joist). The following equation represents the mass transfer boundary condition.

$$P_S = P_\infty \quad (5)$$

Where P_S is the surface pressure and P_∞ is ambient pressure.

Source Terms

In order to simulate the chemical reactions that take place in the materials, namely calcination in gypsum board and pyrolysis in wood, Arrhenius expressions are used where the Arrhenius expression's constants have been determined through thermal gravimetric analysis (TGA) [10]. Evaporation is modelled assuming the partial pressure of water inside the material is always at the equilibrium vapour pressure, which is a function of temperature [8].

Material Properties

The material properties used in the model have been reported in a previous paper [8]. However, the permeability of gypsum board has been changed to 3.8×10^{-14} m as reported in [11]. The material

properties used in the model are based on gypsum board and wood species typically used in North America.

EXPERIMENTAL PROGRAM

Two full-scale floor tests were completed at the National Research Council of Canada. The assemblies were tested according to ASTM E119 [2] with one exception. The second test used a more realistic temperature-time curve that was based on temperature measurements in experiments conducted in fully furnished wood-frame houses [12]. A comparison between the two exposures is shown in Fig. 2.

The full-scale floor assembly was 4.86 m by 3.95 m and loaded to its full design load during the tests. The floor assembly chosen for model validation consisted of solid wood joists 38 mm by 235 mm spaced at 406 mm on centre and protected by two layers of 12.7 mm Type C gypsum board screwed directly to the wood joists. The sub-floor consisted of two layers of 15.9 mm tongue and grove plywood nailed to the joists. Cross-bracing was installed at mid-span and the cavities were not insulated. A total of 102 thermocouples were installed in the floor assembly.

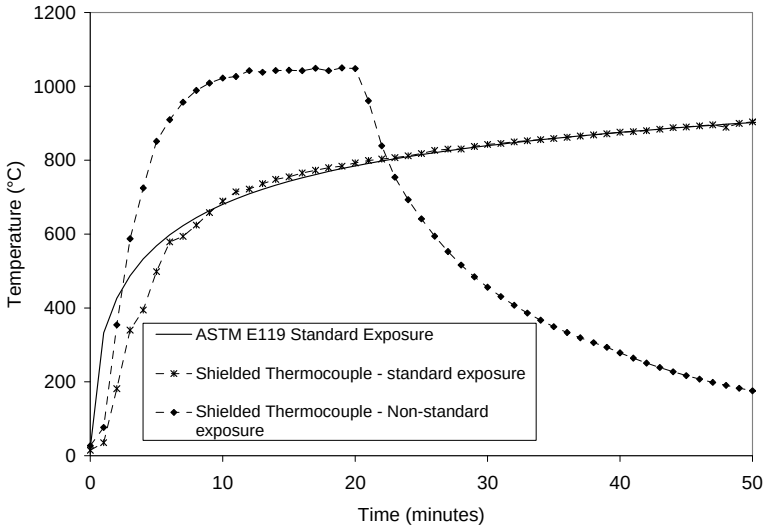

Fig. 2. Comparison between standard and non-standard temperature-time curves used in experiments.

The first full-scale assembly exposed to the standard temperature-time curve failed structurally at approximately 54 minutes. The first layer of gypsum board fell-off at 45 to 48 minutes, while the base layer started to fall off at 50 minutes. The temperature on the back side of the face layer of gypsum board was 600°C when it fell from the assembly, however, the temperature on the back side of the base layer of gypsum board was much lower 250°C – 350°C when it fell from the assembly. The second full-scale assembly exposed to the non-standard temperature-time curve did not fail. The first layer of gypsum board fell-off at approximately 13.5 minutes and exhibited very interesting behaviour before falling off. At approximately 11 minutes, the exposed layer of gypsum board began to spall. The surface of the gypsum board slowly became detached from the core of the board and fell in small pieces. The second layer also started to spall before the furnace was shut down at 20 minutes, although the pieces were smaller. The furnace was then kept closed to allow the temperature to drop slowly. The temperature between the base layer of gypsum board and the wood joist reached approximately 400°C before beginning to cool. The floor subjected to the non-standard exposure did not fail and actually "self-extinguished" after approximately 60 minutes.

RESULTS AND DISCUSSION

The first step in accurately simulating the experiments is to determine the boundary conditions the floor assembly is exposed too. While the furnace used can accurately follow the time-temperature curve specified in the standard [3], the actual temperature inside the furnace is not known. This is because

shielded thermocouples that have a time constant of 5.7 to 7.2 minutes [3] are used to measure the temperature inside the furnace. Therefore, in the first 10 minutes of the test, the temperature in the furnace is considerably higher than what the shielded thermocouples are reading. Researchers at the National Research Council of Canada carried out a series of tests where both shielded thermocouple and plate thermometer measurements were taken [14]. Since the plate thermometer has a much smaller time constant (on the order of one minute), it provides a more accurate measurement of the actual temperature in the furnace than the shielded thermocouples. This is especially true in the first 10 minutes of the test. In Fig. 3 below, the shielded thermocouple, standard exposure [3], and the plate thermometer measurements are compared (note that since the plate thermometer data was not available, the data points were read from the graph published in [14] and, therefore, may not be exact).

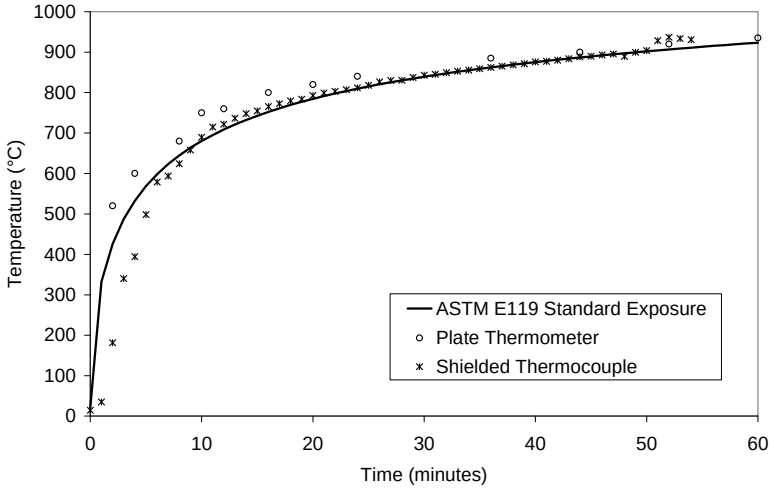

Fig. 3. Comparison between standard temperature exposure [3], shielded thermocouple measurements and plate thermometer measurements.

Since the plate thermometer measurements are closer to the actual temperature in the furnace, a curve was fit to these data points and used as the furnace temperature for the simulation of the standard exposure experiment. Unfortunately, since the temperature-time curve used in the non-standard exposure was unique, there are no data to provide guidance on the actual temperature in the furnace other than the results from the standard exposure. Therefore, the temperature difference between the plate thermometers and the shielded thermocouples was applied to the non-standard shielded thermocouple measurement with the understanding that the temperatures in the furnace are under predicted.

Full-scale Standard Exposure Comparison

Model predictions are compared to the thermocouple measurements at locations one through seven found in Fig. 4. At each location in Fig. 4, there were between 3 and 9 thermocouples placed at different points in the floor assembly. Each thermocouple is plotted in order to provide some insight into the variability at different locations within the floor assembly. None of the thermocouple measurements presented in this paper were located close to joints in either the face layer or the base layer of gypsum board. Thermocouples 1, 2, 4, 6, and 7 were all centred between two joists with TC4 in the geometric centre of the cavity. Thermocouple TC3 was placed on the surface of the joist between the gypsum board and joist and TC 5 was placed in a hole drilled from the side of the joist so that it was in the geometric centre of the joist cross-section.

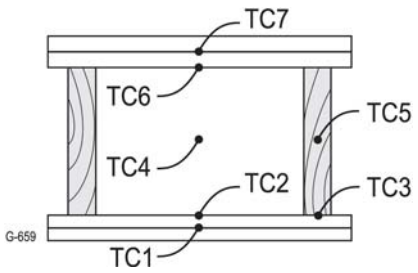

Fig. 4. Thermocouple locations used in comparison between model predictions and experiment.

In the following figures, which compare model predictions to experimental measurements from the standard exposure test, the bold solid line indicates the temperature predicted by the model. Lines at 45 minutes and 50 minutes indicate when the first and second layers of gypsum board begin to fall off the assembly. Note that the model does not account for the falling off of the gypsum board and therefore predictions should only be compared up to the point of fall-off (45 minutes – 50 minutes).

The temperature between the face layer and base layer of gypsum board (TC1 in Fig. 4) is shown in Fig. 5. The model predictions compare favourably with the temperature measurements. In particular, the point at which calcination of the gypsum is complete in the first layer of gypsum board and the temperature begins to rise rapidly is accurately predicted. The temperature is slightly over predicted after approximately 23 minutes which would suggest the thermal conductivity above 400°C may be over predicted.

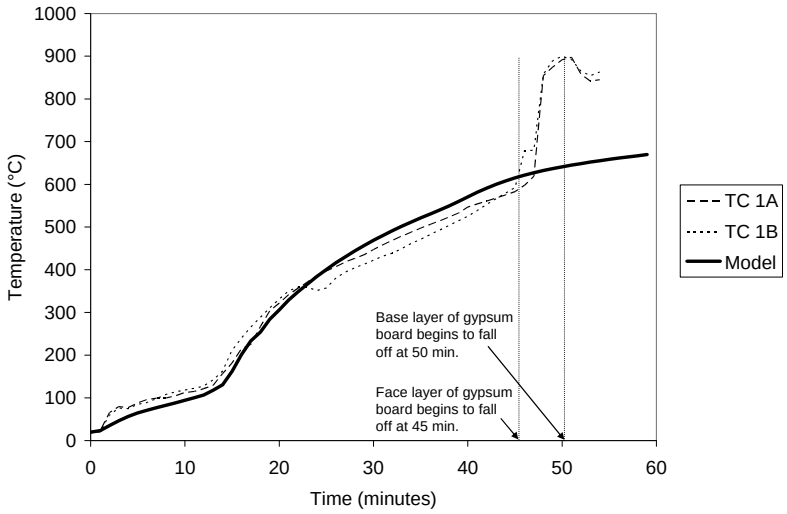

Fig. 5. Comparison between temperatures measured at TC1 and model predictions.

The temperature on the back side of the base layer of gypsum board facing the cavity (TC2 in Fig. 4) is shown in Fig. 6. Again, the temperature is accurately predicted up to 36 minutes where the model predicts calcination is complete. The test results show calcination is complete at 42 minutes. The over prediction of calcination may again be due to over prediction of the thermal conductivity at higher temperatures and therefore the over prediction of the heat flux through the face layer of the gypsum board. The steep rise in the predicted temperature after calcination is complete in the base layer is further evidence that the thermal conductivity of the gypsum board at higher temperatures is over predicted.

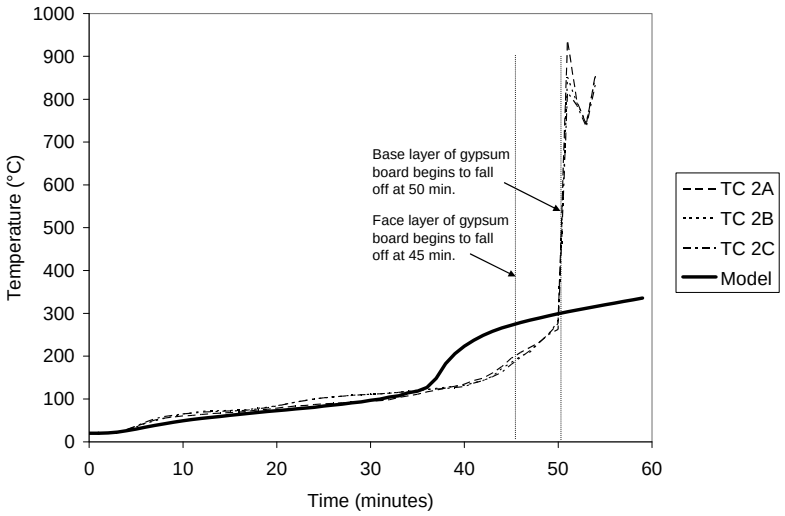

Fig. 6. Comparison between temperatures measured at TC2 and model predictions.

The temperature between the back side of the base layer of gypsum board and the solid wood joist (TC3 in Fig. 4) is shown in Fig. 7. Similar to the previous location, the rate of calcination of the base layer of gypsum board is over estimated, therefore showing a temperature rise after the plateau approximately six minutes earlier than measured.

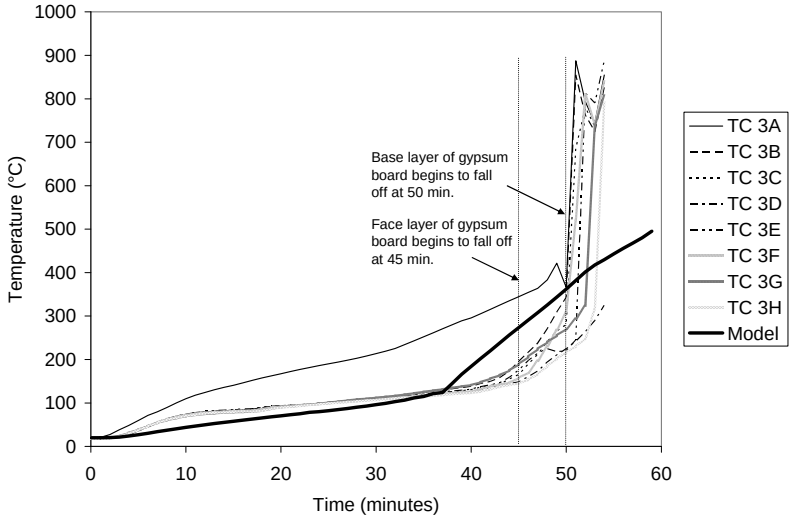

Fig. 7. Comparison between temperatures measured at TC3 and model predictions.

The temperature in the cavity (location TC4 in Fig. 4) is shown in Fig. 8. The temperature in the cavity is under predicted until the gypsum board is fully calcinated at which point the predicted temperature rises quickly. The over prediction of the temperature on the unexposed side of the gypsum board is what causes the predicted temperature in the cavity to quickly rise at 37 minutes. The under prediction in the first 40 minutes is most likely due to the assumption made in the model that the gas in the cavity is fully transparent. Thus, the heating of the gas due to radiation is not accounted for. Also, any mass transfer that enters the cavity from the gypsum board is not taken into account in the model. With this location, there is also some uncertainty as to how accurately the thermocouple is reading the gas temperature when it is also seeing radiation from the gypsum board which would cause the thermocouple to read a higher temperature.

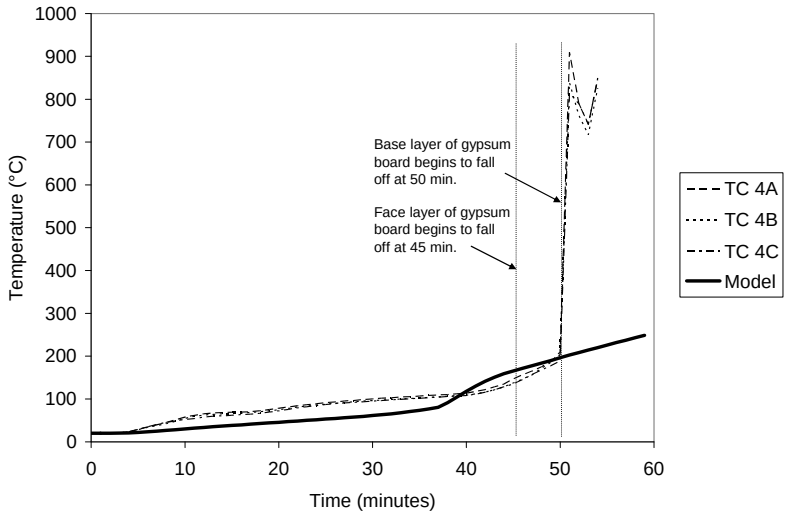

Fig. 8. Comparison between temperatures measured at TC4 and model predictions.

The temperature on the bottom surface of the sub-floor exposed to the cavity (location TC5 in Fig. 4) is shown in Fig. 9. The temperature is under predicted for the entire test. This is in part due to the under prediction of the temperature of the gas in the cavity.

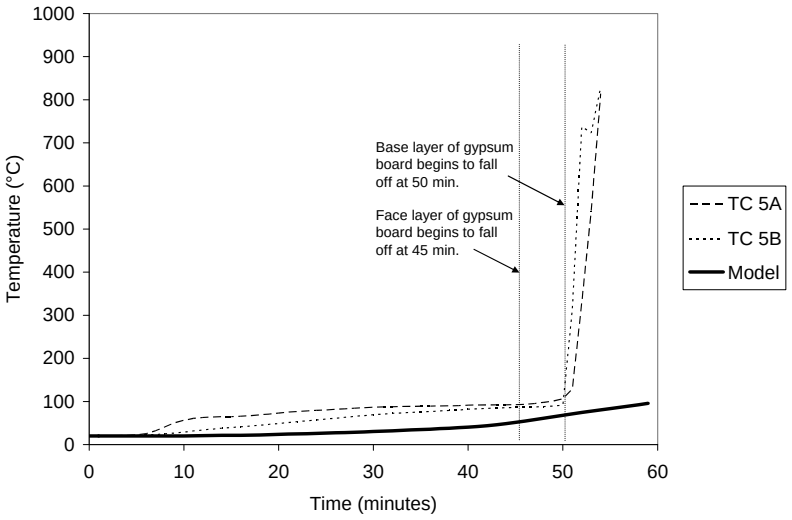

Fig. 9. Comparison between temperatures measured at TC5 and model predictions.

The temperature in the centre of the joist (TC6 in Fig. 4) is shown in Fig. 10. The temperature is underestimated by the model until approximately 40 minutes. This is most likely due to the underestimation of the temperature in the cavity since the heat transfer to the centre of the joist would be dominantly from the side of the joist.

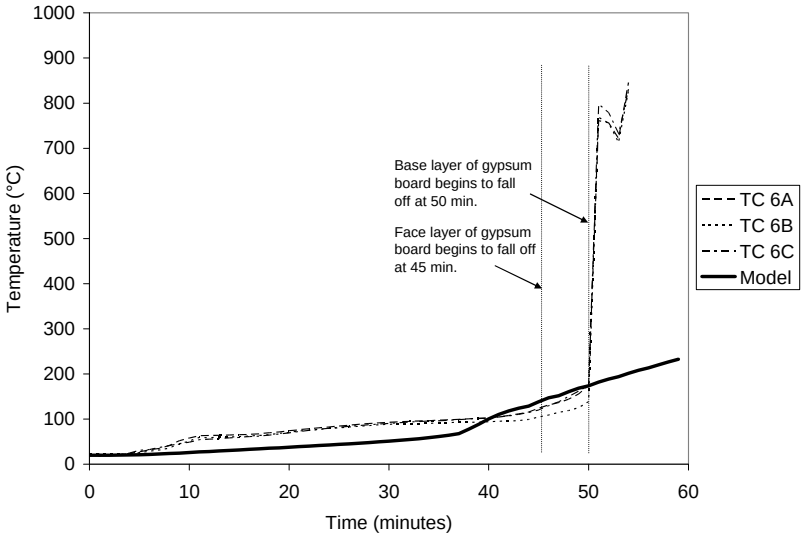

Fig. 10. Comparison between temperatures measured at TC6 and model predictions.

The temperature between the two layers of plywood sub-floor (TC7 in Fig. 4) is shown in Fig. 11. The temperature is slightly underestimated for a large part of the test before closing the gap near the end. After reviewing the temperature on the underside of the sub-floor, this would be expected.

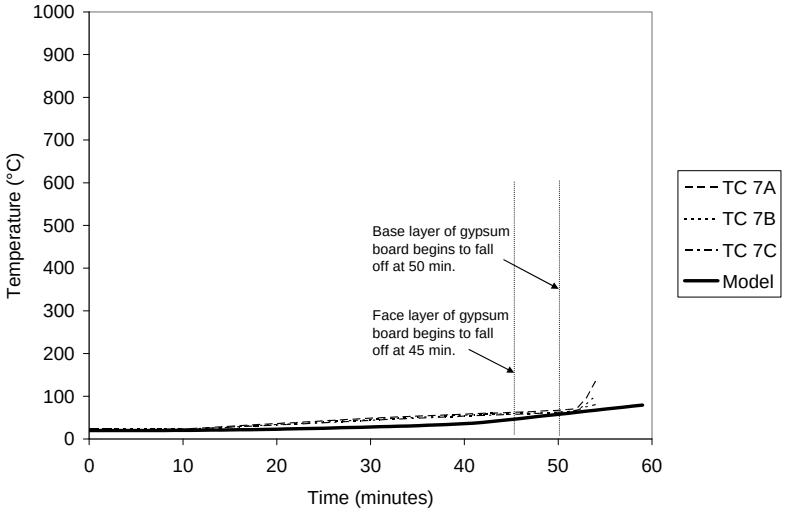

Fig. 11. Comparison between temperatures measured at TC7 and model predictions.

Full-scale Non-standard Exposure Comparison

Model predictions are compared to the full-scale non-standard exposure test below in Fig. 12. Since the time to fall-off of the first layer of gypsum board was only 13 minutes, and the model is unable to simulate this, only the temperatures between the two layers of gypsum board and the back side of the gypsum board will be looked at. Between the two layers of gypsum board, the point at which calcination is complete is accurately predicted. However, the initial rise during calcination is not predicted by the model. As stated previously, both the first layer of gypsum board as well as the second layer exhibited non-explosive spalling which would reduce the thickness of the gypsum board. This is not replicated in the model. Also, the falling off of the first layer of gypsum board at 13 minutes is not reflected in the model. Even with

these shortcomings of the model, the point at which calcination of the second layer is complete is closely predicted.

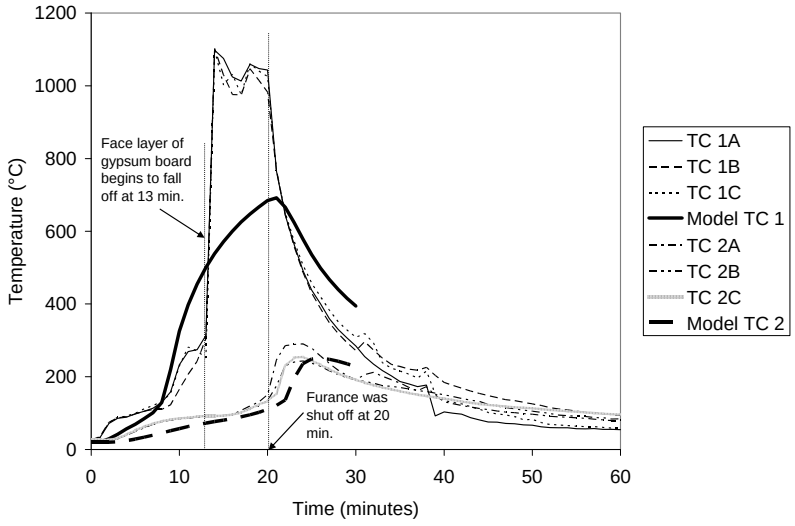

Figure 12. Comparison between temperatures measured at TC 1 and TC2 in the non-standard exposure test and model predictions.

CONCLUSIONS AND FUTURE WORK

A heat and mass transfer model has been presented that uses a finite-element analysis to solve for temperature and pressure across a two-dimensional domain. Calcination of gypsum board and pyrolysis of wood are modelled using Arrhenius expressions and evaporation is modelled based on the equilibrium vapour pressure. The gas in the cavity is assumed to be fully transparent.

Model predictions compare well with data generated in the two full-scale experiments. Given the depth of the floor assembly, a significant amount of the heat transfer is through the cavity by radiation and convection. Until the base layer of gypsum board is fully calcinated, the model seems to under predict the heat transfer into the cavity. This is most likely due to the assumption that the gas in the cavity is fully transparent as well as the mass transfer that leaves the gypsum board and enters the cavity is not accounted for in the model.

While the model's results are encouraging for the non-standard exposure, more work is needed to better quantify the temperature in the furnace and simulate the fall-off of the gypsum board since it occurs so early in the exposure. An attempt will also be made to determine if the pressure in the gypsum board can be linked to the spalling-like behaviour observed in the test.

Future efforts will be directed towards improving the material properties data of gypsum board and wood at elevated temperatures.

ACKNOWLEDGEMENTS

FPInnovations – Forintek Division would like to thank its industry members, Natural Resources Canada (Canadian Forest Service), and the Provinces of British Columbia, Alberta, Saskatchewan, Manitoba, Ontario Québec, Nova Scotia, New Brunswick and Newfoundland and Labrador for their guidance and financial support for this research.

This work was partially supported by the Natural Science and Engineering Research Council of Canada and by Materials Manufacturing Ontario.

REFERENCES

[1] George Hadjisophocleous and Zhuman Fu, "Development and Case Study of a Risk Assessment Model CUrisk for Building Fire". Eighth International Symposium on Fire Safety Science, Beijing, China, 2005. doi:10.3801/IAFSS.FSS.8-877

[2] CAN/ULC S101-07, 2007. Standard Methods of Fire Endurance Tests of Building Construction and Materials, Underwriters' Laboratories of Canada, Scarborough, Canada.

[3] ASTM E119-05a, 2006. Standard Test Methods for Fire Tests of Building Construction and Materials, Annual Book of ASTM Standards, Vol. 04.07, ASTM, Philadelphia, pp. 331-51.

[4] Mehaffey, J.R., Cuerrier, P., and Carisse, G. 1994. A Model for Predicting Heat Transfer through Gypsum-Board/Wood-Stud Walls Exposed to Fire. Fire and Materials (18), pp. 297-305. doi:10.1002/fam.810180505

[5] Takeda, H. and Mehaffey, J.R. 1998. WALL2D: a model for Predicting Heat Transfer through Wood-Stud Walls Exposed to Fire. Fire and Materials 22, 133-140. doi:10.1002/(SICI)1099-1018(1998070)22:4<133::AID-FAM642>3.0.CO;2-L

[6] Clancy, P. 1999. Time and Probability of Failure of Timber Framed Walls in Fire. PhD Thesis, Victoria University of Technology, Victoria, Australia.

[7] Thomas, G.C. 1997. Fire Resistance of Light Timber Framed Walls and Floors. PhD Thesis, School of Engineering, University of Canterbury, Christchurch, New Zealand.

[8] Craft, S., Mehaffey, J., Hadjisophocleous, G. and, Isgor, B. 2007. Modelling the Heat and Mass Transfer in Light-frame Wood Floor Assemblies Exposed to Fire. Proceedings of the Interflam 2007, 11th International Fire Science and Engineering Conference, September 3rd - 5th, 2007, London, UK.

[9] Fredlund, B. 1998. A Model for Heat and Mass Transfer in Timber Structures During Fire. Ph.D. Dissertation, Lund University, Sweden.

[10] Craft, S.T., Hadjisophocleous, G., Isgor, B., and Mehaffey, J. 2006. Predicting the Fire Resistance of Light-frame Wood Floor Assemblies. Proceedings of the 4th International Workshop Structures in Fire. Aveiro, Portugal. pp. 936-950.

[11] Bjork, F., Lundblad, D, Odeen, K. 1997. Transport of Air, Tracer Gas and Moisture Through a Cellulose Fibre Insulated Structure. Nordic Journal of Building Physics 1, 1 – 10.

[12] Mehaffey, J.R., Craft, S.T. and Richardson, L.R. 2004. Analysis of Fire Experiments Conducted in Wood-frame Houses. Proceedings of the 5th International Scientific Conference Wood and Fire Safety, Štrbské Pleso, Slovak Republic.

[13] Ball, M.C. and Norwood, L.S. 1969. Studies in the System Calcium Sulphate-Water. Part I. Kinetics of Dehydration of Calcium Sulphate Dihydrate. J. Chem. Soc. (A) 11, 1633.

[14] Sultan, M.A. 2006. Fire Resistance Furnace Temperature Measurements: Plate Thermometers vs Shielded Thermcouples. Fire Technology, 42, 253-267. doi:10.1007/s10694-006-8431-7